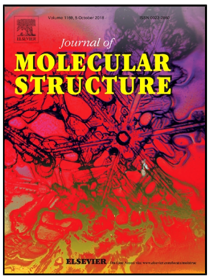

Spectroscopic characterization and photophysical properties of Schiff base metal complex

N.K. Gondia, S.K. Sharma

PII: S0022-2860(18)30711-7

DOI: 10.1016/j.molstruc.2018.06.010

Reference: MOLSTR 25297

To appear in: *Journal of Molecular Structure*

Received Date: 16 February 2018

Accepted Date: 04 June 2018

Please cite this article as: N.K. Gondia, S.K. Sharma, Spectroscopic characterization and photophysical properties of Schiff base metal complex, *Journal of Molecular Structure* (2018), doi: 10.1016/j.molstruc.2018.06.010

Spectroscopic characterization and photophysical properties of Schiff base metal complex

N. K. Gondia and S. K. Sharma*
Department of Applied Physics, Indian Institute of Technology (Indian School of Mines),
Dhanbad 826004, India
*Corresponding author E mail: sksharma.ism@gmail.com
Tel: +91-326-2235412; Fax: +91-326-2296563

Abstract:

In the present work, Schiff base ligand N,N-bis(salicylidene)-(3,3'-diaminobenzidine) and its zinc complex were synthesized. The coordination of Schiff base ligand with zinc metal ion seems to occur via N- azomethine followed by the deprotonation of OH group. The nuclear magnetic resonance peaks as well as important bands in the Fourier transform infra-red spectra are discussed in relation to the structure of the ligand and complex. The optical properties like absorption and fluorescence were studied to get the idea about the transition among molecular orbitals as well as quantum yield. Colour coordinates of complex fall in the blue region. HOMO-LUMO energy gap was used to determine various parameters. Thermal studies were also performed to determine the thermal stability of the complex in the range from room temperature to 500ºC.

Keywords: Schiff base**,** Absorption, Fluorescence, HOMO-LUMO

1. INTRODUCTION

During the past decades metal complexes of Schiff base are widely studied due to having good luminescence properties, high conductivity and thermal stability. Schiff-base ligands coordinated with metals usually linked to the imine nitrogen and aldehyde group. Luminescence properties of the aromatic bridged azomethine metal complexes have already been reported. Among many of the coordination compounds, zinc metal based Schiff base complexes have been found to show the good luminescence properties due to d^{10} electronic configuration [1,2]. Salicylaldehyde schiff base Zn complex generally exhibit photoluminescence as well as electroluminescence properties and formed the basis of materials used in various display and lighting devices either as electron transport layer or emissive layer.

The structures of salicylaldehyde Schiff bases are similar to those of 8-hydroxyquinoline ligands, which have at least one hydroxyl group, a coordination nitrogen atom and a delocalized system. The salicylaldimine ligand forms the basis of an extensive class of chelating ligands that has very popular use in the coordination chemistry of transition and main group elements [3]. Metal complexes particularly having transition metal ions at inner coordination sphere play an important role in achieving color tunable properties with high value of luminous efficacy of radiation [4,5]. Schiff base complexes of transition and non-transition metals have been used extensively for various optoelectronic applications due to their ease of synthesis, wide range of complexation ability and many useful properties like electron transportation, higher thermal stability and ease of sublimation. These complexes have ability to show the tunable properties by varying the substituent derivatives of the coordinated metal ion and enhance their activities [6].

The fluorescence intensity and quantum yield of metal complexes change with respect to ligand after complexation with various metals. The coordination complex derived from condensation reaction of diamines and salicylaldehyde generally exhibit good luminescence properties [7] and can be used as light emitting material in organic light emitting diodes and fluorescent sensors.

The addition of electron donating group into the salicylidene moiety of Zn(II) complex results in the enhancement of quantum yield and emission of light in blue region [8-10].

Efforts have been put to develop a new cost effective material with ease of synthesis and good luminescent properties. The present work describes the synthesis and spectroscopic characterization of Zn(II) complex derived from 3,3'-diaminobenzidine and salicylaldehyde. Absorption and fluorescence spectra were recorded to get the quantum yield and CIE parameters. Zn complex was found to exhibit higher luminescence intensity compared to ligand. CIE parameters, results of thermal studies and HOMO-LUMO energy gap suggest the suitability of synthesized complex in organic light emitting devices.

2. EXPERIMENT

The reagent used in the present studies 3,3'-diaminobenzidine and salicylaldehyde were purchased from Sigma Aldrich. Zinc nitrate was purchased from Merck chemical company. Ethanol was used as a solvent. All the solvents and metal salt were used without further purification. The Schiff-base ligand and its zinc complex were synthesized by the condensation reaction method.

2.1 Synthesis of ligand and complex

3,3'-diaminobenzidine (100 mg, 0.466 mmol) was dissolved in 20 ml of ethanol in a round bottom flask. Salicylaldehyde (0.198 ml, 1.866 mmol) was added with continuous stirring. The mixture was refluxed for three hours and then allowed to cool. The final product was collected after filtration and orange colour Schiff base ligand N,N–bis(salicylidene)-(3,3'-diaminobenzidine) was obtained.

The zinc complex was prepared by mixing the synthesized ligand (50 mg, 0.079 mmol) in ethanol (20 ml) and zinc nitrate (30.02 mg, 0.158 mmol) with continuous stirring [11]. The yellow precipitates confirm the formation of complex. These precipitates were filtered and washed several times with ethanol and then dried over silica gel to obtain the desired complex. The following are the proposed structures (Fig.1 and Fig.2) of the prepared ligand and complex:

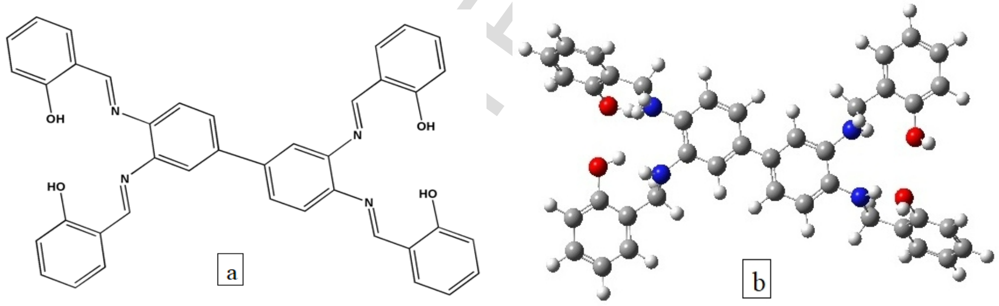

Fig.1 (a) Chemical structure **(b)** Optimized molecular structure of ligand

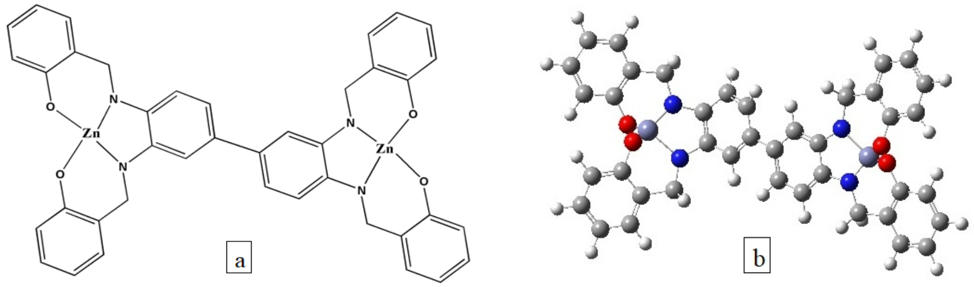

Fig.2 (a) Chemical structure **(b)** Optimized molecular structure of complex

2.2 Measurements:

Fourier Transform Infra-red spectra were obtained in KBr background in the wave number range 4000-400 cm^{-1} using Perkin Elmer make spectrum RX1 FTIR 2000 spectrometer. Nuclear Magnetic Resonance spectra were recorded on JEOL JNM-EXCP 400 MHz NMR spectrometer. Absorption spectra were obtained on Agilent Cary 5000 UV-VIS NIR spectrophotometer. Fluorescence emission spectra were measured on Hitachi F-2500 Fluorescence spectrophotometer in the wavelength range 200-800 nm. HOMO-LUMO and other quantum chemical parameters were computed by Gaussian computational chemistry program using semi empirical and DFT approach . Quantum yield of ligand and complex was calculated by using the standard quinine sulphate which has a fixed and known fluorescence quantum yield. Photometric parameters were calculated using colour calculator programme developed by Osram Sylvania.

3. RESULTS AND DISCUSSION

3.1 FTIR Studies

The Fourier Transform Infra-red (FTIR) spectra of ligand and complex are shown in Fig.3. The positions of functional groups for the prepared ligand and complex are listed in Table 1. The absorption band at 1613 and 1610 cm^{-1} in ligand and complex is due to presence of azomethine group. Bands at 3460 and 3425 cm^{-1} are due to presence of water molecule. A slight shift in peak position was observed after complex formation. The shifting of bands corresponding to nitrogen atom of amine (azomethine) group, hydroxyl group of salicylaldehyde and C-H indicates the coordination of metal to the ligand resulting formation of complex [12-13].

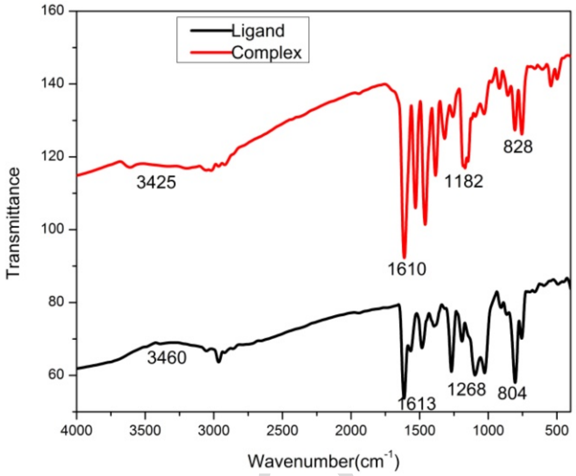

Fig.3 FTIR spectra of ligand and complex

Compound	O-H	C=N	C-OH	C-H
Ligand	3460	1613	1268	804
Complex	3425	1610	1182	828

Table 1: Position of functional groups (cm^{-1}) in FTIR spectra

3.2 NMR Studies:

The Nuclear Magnetic Resonance (NMR) spectra of ligand and complex (Fig.4 & Fig.5) were obtained with DMSO as a solvent. In HNMR spectra it was found that the OH signal, which appears at 13.02 ppm in the ligand gets disappear in the complex indicating removal of OH proton during chelation process with metal ion. Two doublets appears at d 7.69 (H), 7.63 (H) belong to the aromatic proton of benzidine after complexation both shifted to 7.86 (H), 7.45(H) slightly and downfield and upfield respectively. Two triplets at 7.93 (H), 7.43 (H) ppm are originating from salicyl moiety. Two doublets and one singlet appear at multiplet 7.01 (H) ppm of salicyl and benzidine moiety respectively [14,15]. The proton signals obtained for ligand and complex were found to be in the expected region and shows good agreement with the values obtained for HC = N and –OH signals.

In ^{13}C spectrum of ligand, carbon signal appear at 163.70 (C-N), 143.02, 141.45, 138.45, 133.52 and 132.55 ppm which indicate the carbon signals of benzidine moiety, 164.80 (C-O), 160.43 (C=N), 125.80, 120.09, 119.36, 117.97 and 116.68 ppm indicate to the carbon signal of salicyl moiety. After complexation with Zn(II), ^{13}C signal shifted to upfield and downfield which appeared at 172.35, 163.46, 162.57, 139.76, 138.49, 136.29, 134.40, 125.65, 123.12, 119.49, 116.87, 114.54 and 113.00 ppm. The chemical shift is the change in position of signals in NMR spectra. Nuclei which exhibit downfield shift feel stronger magnetic field due to the removal of electron density whereas upfield shift in nuclei indicate the addition of electron density.

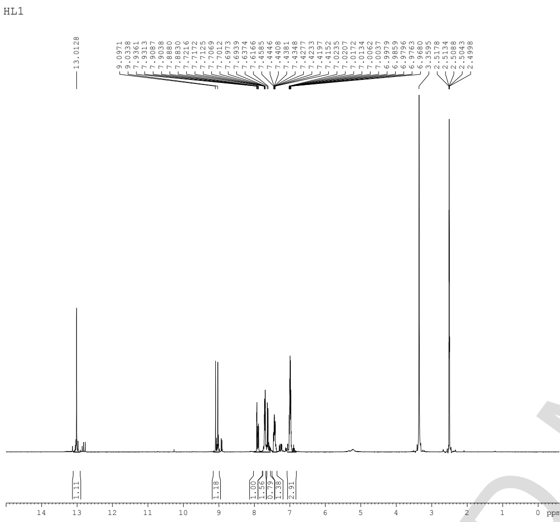

Fig.4 (a) HNMR spectra of Ligand

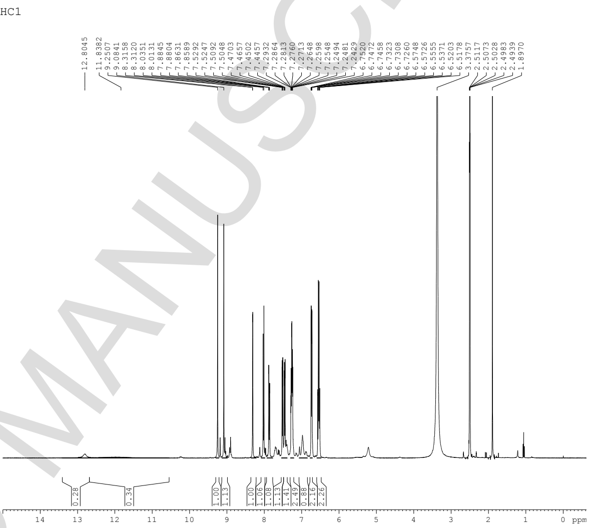

Fig.4 (b) HNMR spectra of complex

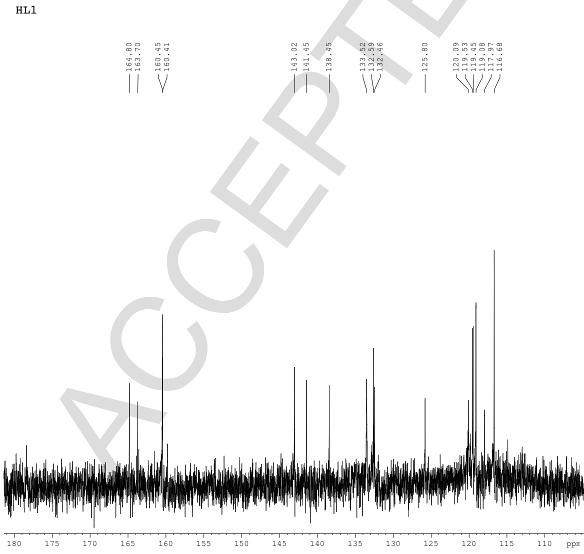

Fig.5 (a) CNMR spectra of Ligand

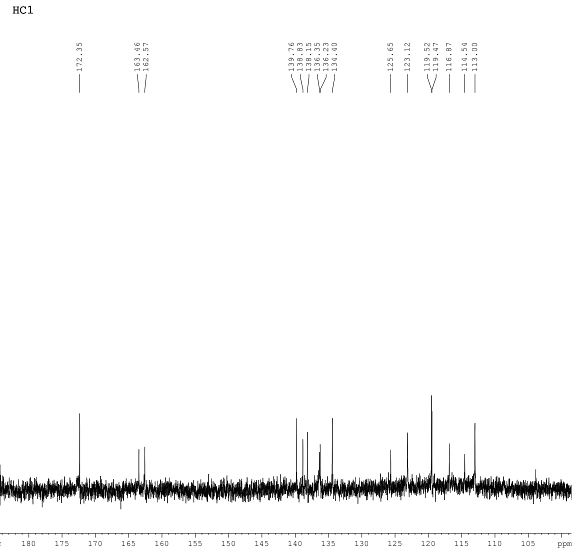

Fig.5 (b) CNMR spectra of complex

3.3 FESEM and EDX Studies:

Field Emission Scanning Electron Microscope (FFSEM) images and Energy Dispersive X-ray (EDX) spectra of ligand and complex are shown in Fig.6 (a, b). The ligand shows a rod like morphology. The complex shows fiber like shape with variable diameter. Significant change in surface morphology was observed after introduction of zinc ions [16]. It was observed that the rod diameter decreases after formation of complex. The EDX spectra were used to measure the elemental composition of C, N, O and Zn in the synthesized ligand/complex [17] and the values in atomic /weight percentage are shown in Table 2.

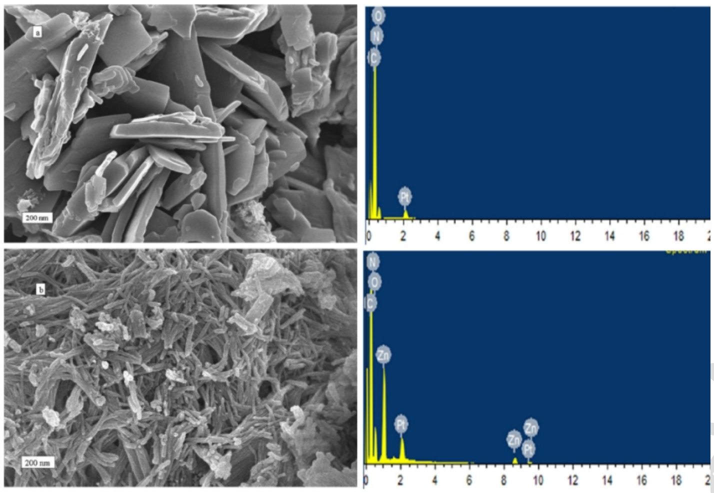

Fig.6 FESEM images and EDX spectra of **a)** Ligand **b)** complex

Ligand	Element	Wt%	Atomic%
	C	67.06	76.62
	N	7.73	7.57
	O	17.83	15.29
Complex	C	50.58	70.49
	N	6.21	7.42
	O	15.80	16.53
	Zn	18.83	4.82

Table: 2 Elemental composition of ligand and complex

3.4 TEM Studies

TEM studies were performed in order to get the idea of particle size and morphology. TEM images of ligand and complex are shown in Fig. 7 (a, b). These images show the change in morphology and particle size after complex formation. The agglomeration of particles are observed in case of complex. The average particle size of ligand and complex was found to be 130 and 60 nm respectively.

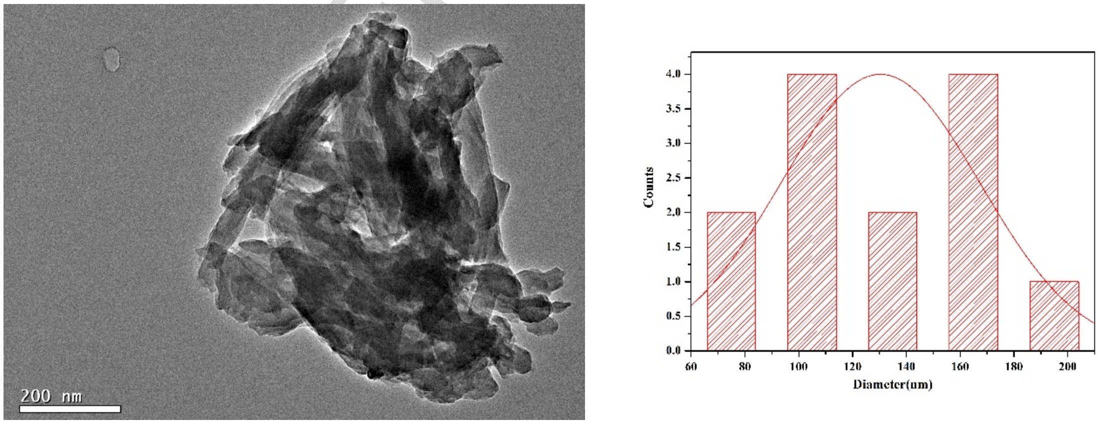

Fig.7 (a) TEM image and size distribution of ligand

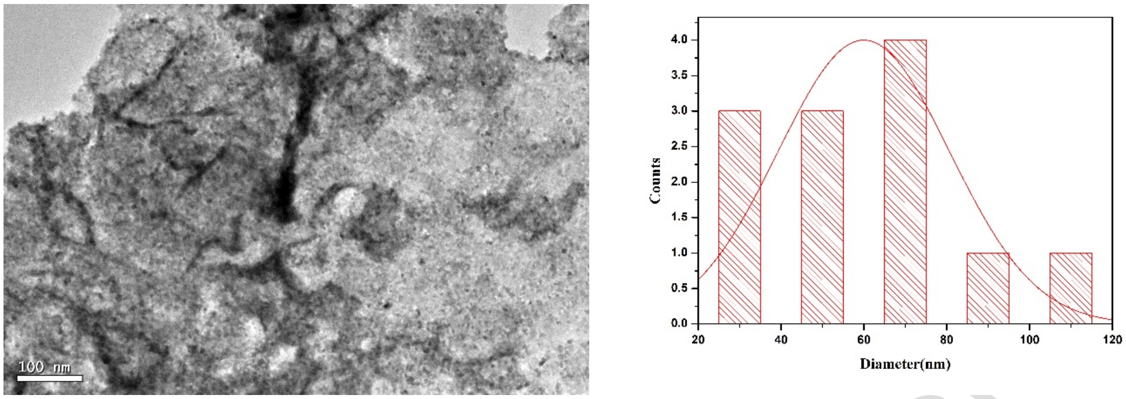

Fig.7 (b) TEM image and size distribution of complex

3.5 UV- Vis studies:

The electronic spectra of ligand and complex in the UV-visible region were recorded in DMSO solvent with 10-^{2} M concentration and the bands assigned are shown in Fig. 8. The absorbance bands in the spectrum of ligand observed at 274 nm and 350 nm are due to n-π* transition of lone pair of electron of azomethine group and anti-bonding π orbital. After coordination, significant bathochromic shift was observed in the spectrum of Zn complex. The Zn complex, shows shifting of band towards red region and were observed at 311 nm and 420 nm. Slight shift in the position of these bands was observed as a result of complexation. This red shifting of band is an indication of intermolecular charge transfer in complex due to π electron conjugation between ligand and Zn^{2+} ion [18,19]. Shifting of absorption bands from 274 nm (ligand) to 311 nm (complex) and 350 nm (ligand) to 420 nm (complex) are due to the participation of lone pair electrons of azomethine nitrogen and conjugation effect with π bond of benzene ring. This is due decrease in energy which cause bathochromic shift. This shifting of bands also confirm the formation of complex from its ligand.

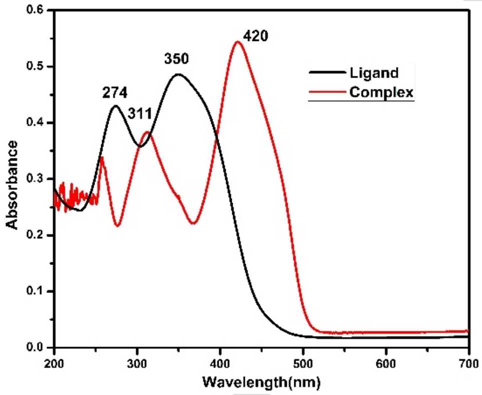

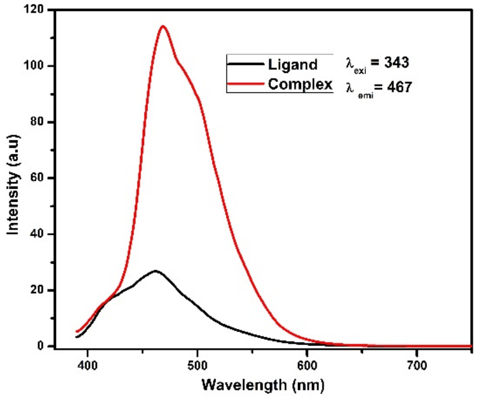

Fig.**8** UV-Vis spectra of ligand and complex **Fig.9** Fluorescence spectra of ligand and complex

3.6 Fluorescence studies

The fluorescence spectra of ligand and complex (Fig.9) were recorded at room temperature in the range 400-800 nm. Both the developed compounds show intense blue emission after excitation with 343 nm wavelength source. The fluorescence emission intensity of complex is higher than the ligand. This increase in intensity is due to the chelation of ligand to metal ion center.

Chelation of ligand to metal ion via complexation results an increment in rigidity of complex and hence loss of energy reduces [20]. This is due to the occurrence of less number of non-radiative intraligand transitions from excited state to ground state.

The fluorescence intensity of ligand may probably be quenched by the occurrence of a photo induced electron transfer (PET) process due to the presence of lone pair of electrons in the ligand. PET is a process in which an excited electron is transferred from donor to acceptor. After the electron transfer, fluorescence intensity of acceptor is quenched due to formation of radical anion. PET process is prevented after the complex formation which results intensity enhancement by the coordination of Zn(II) ions.

3.7 Quantum yield:

The fluorescence quantum yield (ϕ) of ligand and complex was calculated by comparative William's method using the following equation [21,22]. The detail can be seen in the previous work by authors [23].

$$\phi_S = \phi_{ST} \frac{m_S\, \eta_{S2}^2}{m_{ST} \eta_{S1}^2}$$

Here, the terms m_S and m_{ST} represent the slopes of samples and standard reference. η_{S1} and η_{S2} are the refractive index of solvents (H_2SO_4 and DMF). The integrated fluorescence intensities were plotted as a function of concentration of ligand, complex and standard reference quinine sulphate. The slopes of curves were calculated to obtain the quantum yield (Fig. 10). Slope and quantum yield values of ligand and complex are tabulated in Table 3.

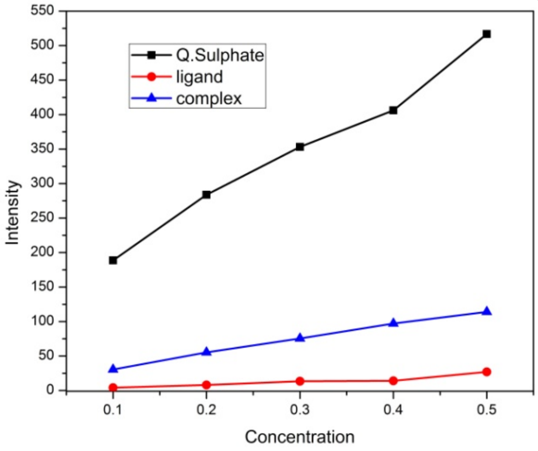

Fig.10 Plot of concentration vs intensity of ligand, complex and standard

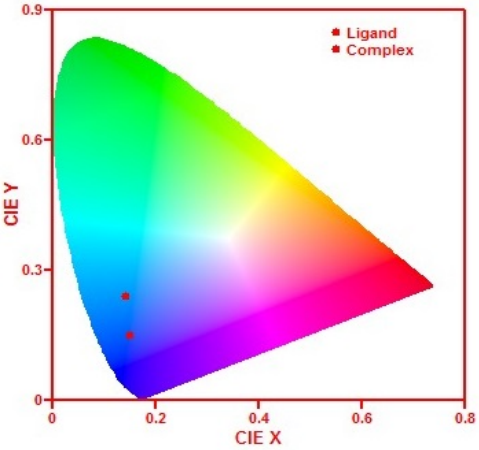

Fig. 11 Chromaticity diagram of ligand and complex

3.8 CIE parameters:

The International Commission on Illumination (CIE) suggested a set of parameters in order to quantify the colour emission from a material using chromaticity diagram. In the present work, this diagram (Fig. 11) was plotted using colour calculator software. Photometric characteristics of prepared ligand and complex were studied from this diagram. Colour coordinates (x, y) for both compounds fall in the blue region with luminous efficacy of radiation (LER) values as shown in Table 3. High value of LER is always favorable for application of a complex in various display devices.

Compound	**Slope**	**Quantum yield**	**Color coordinates**		**LER (lm/w)**
			x	**y**	
Ligand	51.72	3.77	0.15	0.15	139
Complex	209.13	15.28	0.14	0.24	206
Standard	777.95	0.54	-	-	-

Table: **3** CIE parameters of ligand and complex

3.9 Quantum chemical parameters:

The highest occupied molecular orbitals (HOMO) and lowest unoccupied molecular orbitals (LUMO) are the energy levels (Fig.12, 13) known as frontier molecular orbitals (FMO). FMO have been found to play an important role in determining quantum cehmical parameters, electrical and optical properties of organic molecules. The HOMO-LUMO energy gap determines the stability and reactivity of a molecule. It is high for hard molecule and small for soft molecule. Lower value of energy gap indicates the ease of charge transfer within the molecule [24,25]. HOMO-LUMO energies of ligand and complex as well as various quantum chemical parameters calculated using the following relations are given in Table 4:

$$\text{Ionization potential (IP)} = -E_{HOMO}$$
$$\text{Electron affinity (EA)} = -E_{LUMO}$$
$$\text{Electronegativity } (\chi) = (IP + EA)/2$$

Compound	HOMO		LUMO		Energy gap		IP (Semi empirical)	EA (Semi empirical)	χ (Semi empirical)
	Semi-empirical	DFT	Semi-empirical	DFT	Semi empirical	DFT			
Ligand	-0.290	-0.208	-0.057	-0.080	0.233	0.128	0.290	0.057	0.1735
Complex	-0.248	-0.198	-0.185	-0.090	0.063	0.108	0.248	0.185	0.2165

Table:**4** Quantum chemical parameters (in eV) of ligand and complex

The low value of HOMO-LUMO gap of complex indicates its more reactiviy and ease of charge transfer compared to ligand. The low value of ionization potential for complex indicates its weak tendency to remove even the most loosely bound electrons and hence the stability of complex is high. The high value of electron affinity and electronegativity for complex indicate its ability to accept or attract electron easily and help in charge transfer process as well as enhances the electrical conductivity. Small value of HOMO-LUMO gap indicates that the complex is a soft molecule.

Density functional theory (DFT) was also used to calculate the value of HOMO-LUMO gap. For this purpose, basic set 6-31G and calculation method RB3LYP was used. HOMO-LUMO energies of ligand and complex as calculated by DFT approach are shown in Table 4. Figures 12 and 13 show a similar type of plots with a slight variation in HOMO-LUMO structures compared to plots obtained by semi empirical approach. The ground state properties of many-electron system depend on the electron density n(x,y,z). The allowed energy states of many-electron system can be determined. In DFT, the electron density is a function of space and time which deals directly with wave function. The comparison of HOMO and LUMO values calculated by two approaches is not always correct. This is because the HOMO's values are found by the actual states of electronic interactions, while the LUMO's are virtual states and the specification of these states is not always accurate [26].

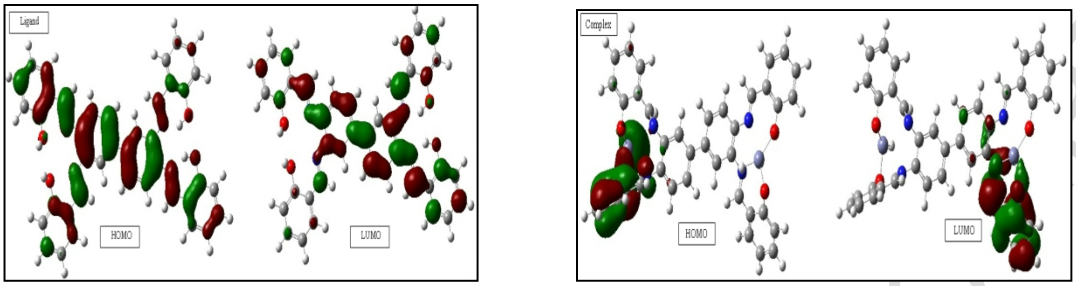

Fig.12 HOMO-LUMO structure of ligand and complex (Semi empirical)

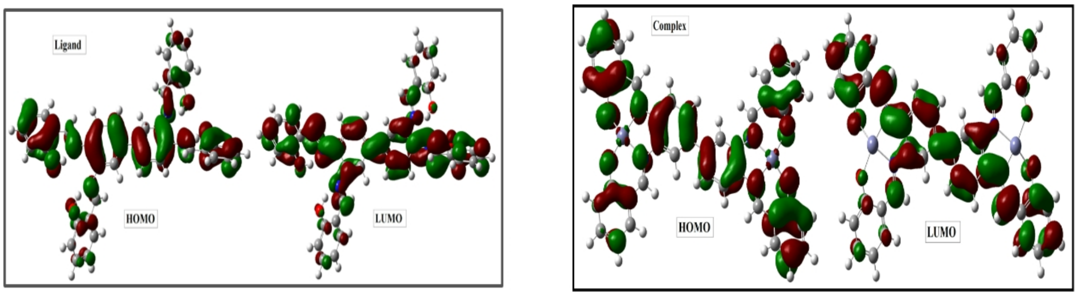

Fig.13 HOMO-LUMO structure of ligand and complex (DFT)

3.10 Thermal studies:

Thermal studies were performed to know about the thermal stability and presence of water molecule with respect to inner coordination sphere of complex. The thermo gravimetric (TG) curve (Fig.13**)** indicates decomposition of complex in three successive stages within the temperature range 100 to 800ºC. The first decomposition in the temperature range 100-250ºC denotes the dehydration process due to removal of water [27-28]. Decomposition of the coordination sphere takes place in the second stage in the temperature range 250-450ºC. The third decomposition in the temperature range 450-800ºC corresponds to the complete loss in mass of the complex. This thermal decomposition is also confirmed by presence of differential thermal analysis (DTA) peaks in the region 100-250ºC, 250-450ºC and 450-800ºC.

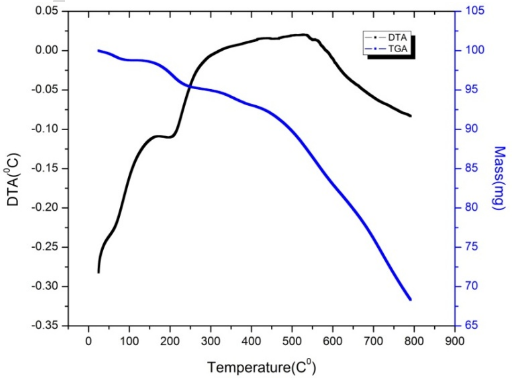

Fig.13 TG/DTA curves of complex

Conclusions:

- NMR studies confirm the coordination of Schiff base ligand with Zn(II) metal ions via N-azomethine group followed by the deprotonation of OH group. The difference in peaks of FTIR spectra of ligand and complex corresponding to C-OH and C=N vibrations indicate the formation of complex. Significant change in surface morphology was observed after inclusion of Zn ions.
- Enhancement in fluorescence intensity, quantum yield and LER after formation of complex suggests its applications in display devices. The color coordinates of complex was observed in the blue region. Low value of HOMO-LUMO gap and thermal stability upto the 500ºC also supports the above application.

Acknowledgement

One of the author Mr. N. K. Gondia gratefully acknowledge the Council of Scientific and Industrial Research (CSIR), New Delhi for awarding him Junior Research Fellowship (Award No 09/085(0110)/2013-EMR-1).

References:

1. S. Basak , S. Sen, S. Banerjee, S. Mitra, G. Rosair, M. T. G. Rodriguez, Three new pseudohalide bridged dinuclear Zn(II) Schiff basecomplexes: Synthesis, crystal structures and fluorescence studies, Polyhedron 26 (17) (2007) 5104-5112.
2. K. H. Chang, C. C. Huang, Y. H. Liu, Y. H. Hu, P. T. Chou, Y. C. Lin, Synthesis of photo-luminescent Zn(II) Schiff base complexes and its derivative containing Pd(II) moiety, Dalton. Trans. 11 (2004) 1731-1738.
3. M. Maiti, S. Thakurta, D. Sadhukhan, G. Pilet, G. M. Rosair, A. Nonat, L. J. Charbonnière, S. Mitra, Thermally stable luminescent zinc–Schiff base complexes: A thiocyanatobridged 1D coordination polymer and a supramolecular 1D polymer, Polyhedron 65 (2013) 6–15.
4. F. Dumur, Zinc complexes in OLEDs: An overview, Synt. Met. 195 (2014) 241-251.
5. M.S. More, S.B. Pawal, S.R. Lolage, S.S. Chavan, Syntheses, structural characterization, luminescence and optical studies of Ni(II) and Zn(II) complexes containing salophen ligand, J. Mol. Struct. 1128 (2017) 419-427.
6. T. Yu, K. Zhang, Y. Zhao, C. Yang, H. Zhang, L. Qian, D.Fan, W.Dong, L.Chen, Y. Qiu, Synthesis, crystal structure and photoluminescent properties of an aromatic bridged Schiff base ligand and its zinc complex, Inorg. Chim. Acta 361 (2008) 233-240.
7. Y. Z. Shen, H. Gu, Y. Pan, G. Dong, T. Wu, X. P. Jin, X. Y. Huang, H. Hu, Synthesis and characterization of dialkylgallium (dialkylindium) complexes of N-salicylidene 2-aminopyridine and N-salicylidene 2-methoxyaniline: crystal structure of dimethyl[N-salicylidene 2-aminopyridine]gallium, J. Org. Chem. 605 (2) (2000) 234-238.
8. H. Temel, H. Hosgoren, New copper(II), manganese(III), nickel(II) and zinc(II) complexes with a chiral quadridentate Schiff base, Tran. Met. Chem. 27 (6) (2002) 609-612.
9. K. Ouari, A. Ourari, J. Weiss, Synthesis and Characterization of a Novel unsymmetrical tetradentate Schiff Base Complex of Zinc(II) derived from N, N-bis (5-

bromosalicylidene) 2,3-Diaminopyridine (H_2L): Crystal Structure of [Zn(II)L]Pyridine, J. Chem. Crystallogr. 40 (10) (2010) 831-836.

10. D. Aiello, L. Malfatti, T. Kidchob, R. Aiello, F. Testa, I. Aiello, M. Ghedini, M. L. Deda, T. Martino, M. Casula, P. Innocenzi, Blue-emitting mesoporous films prepared via incorporation of luminescent Schiff base zinc(II) complex, J. Sol-Gel Sci. Technol. 47 (2008) 283-289.
11. A. Bhattacharyya, S. Roy, J. Chakraborty, S. Chattopadhyay, Two new hetero-dinuclear nickel(II)/zinc(II) complexes with compartmental Schiff bases: Synthesis, characterization and self assembly, Polyhedron 112 (2016) 109-117.
12. S. A. B. Guzzi, H. S. El. Alagi, Synthesis and characterization of Fe(II) and Co(II) complexes of Schiff base derived from 3,3'-diaminobenzidine and salicylaldehyde, J. Chem. Pharm. Res. 5 (10) (2013) 10-14.
13. F. Arslan, M. Odabasoglu, H. Olmez, O. Buyukgungor, Synthesis, crystal structure, spectral and thermal characterization of bis(o-vanillinato)-triethylen glycoldiimine copper(II) and bis[(R)-(-)-hydroxymethylpropylimine o-vanillinato] copper(II), Polyhedron 28 (14) (2009) 2943-2948.
14. G. G. Mohamed, M. M. Omar, A. M. Hindy, Metal Complexes of Schiff Bases: Preparation, Characterization, and Biological Activity, Turk. J. Chem. 30 (2006) 361-382.
15. J. Zhang, G. Dai, F. Wu, D. Li, D. Gao, H. Jin, S. Chen, X. Zhu, C. Huang, D. Han, Efficient and tunable phosphorescence of new platinum(II) complexes based on the donor– Π acceptor Schiff bases, J. Photochem. and Photobio. A: Chem. 316 (2016) 12-18.
16. M. Chowdhury, S. K. Sharma, Spectroscopic behavior of Eu^{3+} in SnO_2 for tunable red emission in solid state lighting devices, RSC Adv. 5 (2015) 51102-51109.
17. S. Das, S. Bhunia, T. Maity, S. Koner, Suzuki cross-coupling reaction over Pd-Schiff-base anchored mesoporous silica catalyst, J. Mol. Catal. A: Chemical 394 (2014) 188-197.
18. R. M. Issa, A. M. Khedr, H. F. Rizk, UV–vis, IR and 1HNMR spectroscopic studies of some Schiff bases derivatives of 4-aminoantipyrine, Spectrochim. Acta Part A 62 (1-3) (2005) 621-629.
19. P. E. Aranha, M. P. D. Santos, S. Romera, E. R. Dockal, Synthesis, characterization, and spectroscopic studies of tetradentate Schiff base chromium(III) complexes, Polyhedron 26 (7) (2007) 1373-1382.
20. B. D. Wang, Z. Y. Yang, Q. Wang, T. K. Cai, P. Crewdson, Synthesis, characterization, cytotoxic activities, and DNA-binding properties of the La(III) complex with Naringenin Schiff-base, Bioorg. & Med. Chem. 14 (6) (2006) 1880-1888.
21. N. Aksuner, E. Henden, I. Yilmaz, A. Cukurovali, A highly sensitive and selective fluorescent sensor for the determination of copper(II) based on a schiff base, Dyes and Pigments 83 (2) (2009) 211-217.
22. M. Martini, M. Montagna, M. Ou, O. Tillement, S. Roux, and P. Perriat, How to measure quantum yields in scattering media: Application to the quantum yield measurement of fluorescein molecules encapsulated in sub-100 nm silica particles, J. Appl. Phys. 106 (2009) 094304.
23. N. K. Gondia, S.K. Sharma, Quantum yield and photometric parameters of some transition metal ion schiff base complexes, Opt. Quant. Electro. 49 (9) (2017) 1-12.

24. X. Ren, J. Li, R. J. Holmes, P. I. Djurovich, S. R. Forrest, M. E. Thompson, Ultrahigh Energy Gap Hosts in Deep Blue Organic Electrophosphorescent Devices, Chem. Mater. 16 (23) (2004) 4743-4747.
25. R.G. Parr, R. G. Pearson, Absolute Hardness: Companion Parameter to Absolute Electronegativity, J . Am. Chem. Soc. 105 (26) (1983) 7512-7516.
26. E. A. Rengifo, G. Murillo, DFT-Based Investigation of the electronic structure of a Double-Stranded AC B-DNA dimmer at different levels of theory, Revista de Ciencias entornogeografico.univalle.edu.co (2012) 117-122.
27. G. B. Bagihalli, P. G. Avaji, S. A. Patil, P. S. Badami, Synthesis, spectral characterization, in vitro antibacterial, antifungal and cytotoxic activities of Co(II), Ni(II) and Cu(II) complexes with 1,2,4-triazole Schiff bases Eur. J. Med. Chem. 43 (12) (2008) 2639-2649.
28. M. E. Behery, H. E. Twigry, Synthesis, magnetic, spectral, and antimicrobial studies of Cu(II), Ni(II), Co(II), Fe(III), and UO_2 (II) complexes of a new Schiff base hydrazone derived from 7-chloro-4-hydrazinoquinoline, Spectrochim. Act. Part A 66 (1) (2007) 28-36.

Highlights

- Synthesis of Schiff base ligands N,N-bis(salicylidene)-(3,3'-diaminobenzidine) and zinc metal complexes.
- Structural, optical, theoretical and thermal studies of ligands and complexes.
- Colour coordinates of complex observed in the blue region.
- Enhancement in fluorescence intensity, quantum yield and LER of complex suggests its applications in display devices.